Journal of Sound and Vibration (1998) **217**(3), 453–466
Article No. sv981780

WHIRL SUPPRESSION IN HAND-HELD POWER TOOL ROTORS USING GUIDED ROLLING BALANCERS

C. Rajalingham and S. Rakheja

Concave Research Center, Department of Mechanical Engineering, Concordia University, Montreal, Québec, Canada

(*Received* 28 *July* 1997, *and in final form* 22 *May* 1998)

Residual unbalance in hand-held power tool rotors transmits undesirable vibrations to the hand of its operator. These vibrations can be effectively suppressed using an automatic balancing element constrained to move in a circular path. In an earlier analysis, the effectiveness of the balancing element on the unbalance rotor vibration suppression was investigated by assuming smooth contact between the balancing element and its guide. The influence of the rolling motion of the balancing element due to friction at the contact is examined in the present study using a three-degree-of-freedom system model in a rotating reference frame. Investigation shows that the rolling motion in a carefully designed balancer improves its stability and its effectiveness in vibration reduction.

1. INTRODUCTION

Hand-held rotary power tools, such as grinders and drills, are known to transmit comprehensive levels of vibration in a wide frequency range to the operator's hand and arm. Prolonged exposure to such vibration has been related to several occupational health disorders, such as tingling, numbness, blancing of fingers, and vibration white finger [1]. The severity of health and safety risks posed by prolonged exposure to hand-transmitted vibration have prompted many clinical and epidemiological studies to identify the primary injury mechanisms, and engineering studies to design vibration isolation mechanisms [2].

The biodynamic response behavior of the human hand–arm to vibration excitations have been extensively investigated to permit development of effective vibration isolators [3, 4]. The studies in vibration isolation mechanisms, however, have been mostly limited to development of resilient handle grips and gloves materials. It has been established that antivibration gloves provide vibration isolation in limited frequency bands, and their effectiveness can be enhanced only at the expense of dexterity loss [5].

The efforts in vibration attenuation of tools, however, have been limited because of their compact design and design complexities. The hand–arm vibration due to hand-held grinders, among various operating factors, are strongly influenced by the residual unbalance forces. The balancing of such tools can yield attenuation

0022–460X/98/430453 + 14 $30.00/0

of hand-transmitted vibration [6]. Furthermore, a class of hand-held power tools with vertical rotors are not significantly influenced by gravitational forces. The rotor of such a power tool can thus be modelled as a single disk flexible vertical rotor supported in rigid bearings for vibration analysis. In this model, the rotor shaft acts as an isotropic elastic support for the disk.

The mass center of the disk, however, does not coincide with the axis of the rotor shaft, due to the residual unbalance. The centrifugal force resulting from the residual unbalance causes the rotor shaft to deflect and to whirl at the synchronous frequency. During the steady whirling motion, the mass center of the disk lies along the radial line joining the center of whirl and the point on the shaft axis where the disk is supported. Further, the center of mass lies outside or in between the whirl center and the disk support point depending on whether the operating speed is below or above the rotor critical speed [7, 8].

In addition to an increase in stresses in the rotor shaft, the unbalance whirling motion introduces dynamic support forces at the bearings also. Direction of force transmitted to the supports changes continuously with the rotating shaft and the vibration induced by this rotating support force is ultimately transmitted to the operator's hand. These vibrations can be minimized using some of the conventional vibration isolation techniques, such as (1) redesigning the rotor such that the operating speed is considerably different from the rotor critical speed, (2) minimizing the unbalance by balancing the rotor, and (3) introducing a vibration absorber on the machine handle.

In an experimental study, Lindell [6] reported the effectiveness of an automatic balancing device for vibration reduction in a hand-held grinding machine. This balancing device consists of several balls constrained to move inside a sealed cylindrical ball–race unit partially filled with oil. A diagram of this balancing device and the details pertaining to its installation in the grinder rotor are also given in this reference. When installed on the rotor, the balls tend to move to a relative rest position in the ball–race under the influence of the centrifugal forces, thereby modifying the effective unbalance of the rotor. In hand-held machine applications where the space limitation is an important design constraint, such an automatic balancing device is a convenient method for the reduction of unbalance induced vibration.

Lindell [6] explained the balancing mechanism of the device with two balls and considered that the balls will move to the precise locations inside the groove to neutralize the rotor unbalance completely. The validity of such an assumption on the rest positions of the balls requires careful consideration. The flexibility of the rotor shaft must also be considered in understanding the balancing mechanism of such a carefully centered balancing device. At the two ball positions, the reaction of the groove on the ball must balance the centrifugal force, which implies that the whirl center must lie on the radial line joining the ball and the groove center. Thus, the two radial lines from the groove center to the ball positions must fall along the same straight line. Consequently, the balls must move either to the same position or to diametrically opposite positions in the groove. Based on this observation, a balancing device with a single ball is considered to be sufficient to study the automatic balancing mechanism of this device.

In an earlier analysis, the authors used a three-degree-of-freedom model, which incorporates flexibility of the rotor shaft in a rotating reference frame, to analyze the stability of these rest positions of the balancing ball [9]. The analysis was further simplified by assuming the contact between the ball and its guide to be smooth. The analysis showed that these ball positions are not always stable. Except for a certain speed range, one of the ball positions is found to be stable. The analysis identified the unstable speed range of the system, which is in the super critical speed range. It showed that the device cannot reduce the unbalance force when the rotor speed is below the critical speed of the system. Further, it revealed the conditions that must be satisfied by the ball mass and groove radius for unbalance vibration reduction at a super critical speed of the system.

Lindell [6] also reported that the balancing device designs for several other applications are not successful and attributed these failures to high rolling friction between the balls and the race. When the balancing element is at one of its rest positions on its guide, the reaction on the roller is in the radial direction, and the frictional force at the contact is zero. A small amount of friction at the contact, however, can introduce a rolling motion of the balancing element for small vibrations about its relative rest position inside the groove. In the present analysis, this rolling motion of the balancing element is carefully considered in the model in order to investigate the role of friction on the effectiveness of the balancing device. The number of degrees of freedom of this improved system model remains the same as that of the earlier model. Further, this analysis can be applied for different balancing elements, such as roller or a ring with smaller radius of gyration than the spherical ball, which can roll easily on the guide.

2. THEORY

A class of hand-held power tools with vertical rotors are not significantly influenced by gravitational forces and the residual unbalance in the disk is the source of excitation. The rotor of such a power tool can be modelled as a single disk flexible vertical rotor supported in rigid bearings for vibration analysis. In this model, the rotor shaft acts as an isotropic elastic support for the disk. The balancing element, which rolls on a concentric guide in the disk influences the whirling motion of the rotor. This influence can be analyzed by studying the motion of the dynamical system composed of the rotor and the balancing device.

A reference frame which rotates at the rotor speed, shown in Figure 1, is chosen to configure the system and to express the equations of motion. The reason for the choice of this rotating reference frame is that the equations of motion expressed in terms of the co-ordinates referred to this frame have time-independent coefficients.

The disk undergoes a translatory motion in this rotating frame and its position is represented by two displacement co-ordinates (x, y) of its support point C on the shaft. The center of the balancing element, which rolls on a concentric circular guide in the disk, is configured using the angular co-ordinate ψ. This three-degree-of-freedom system model is used in the present analysis to study the

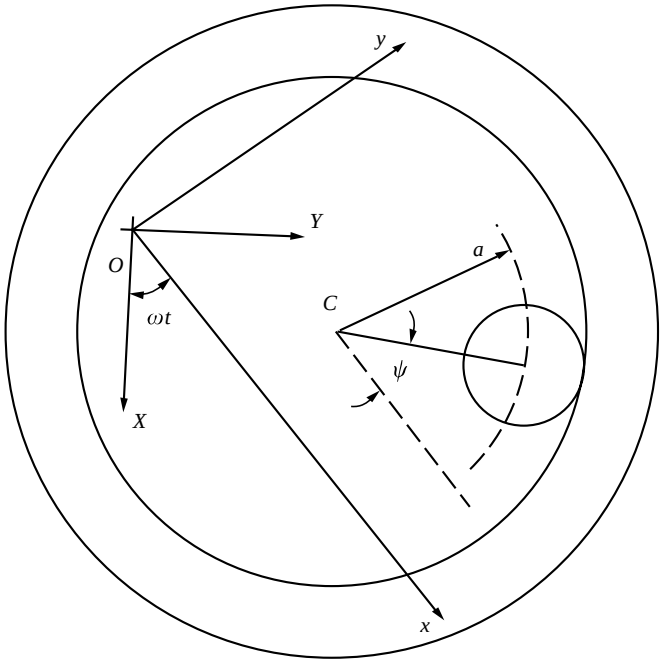

Figure 1. Frame of reference.

influence of rolling motion of the balancing element on the unbalance whirling motion of the rotor.

3. GOVERNING EQUATIONS

The absolute acceleration components in the Ox and Oy directions corresponding to the displacement (x, y) of the rotor center in the rotating frame can be expressed as $(\ddot{x} - 2\omega\dot{y} - \omega^2 x)$ and $(\ddot{y} + 2\omega\dot{x} - \omega^2 y)$, respectively [8]. Relative to the rotor center, the balancing element moves in a circular path of radius a, and its angular position relative to the fixed direction is $(\psi + \omega t)$. Thus, the angular velocity and acceleration of the radial vector in a non-rotating frame located at the rotor center are $(\dot{\psi} + \omega)$ and $\ddot{\psi}$, respectively. Consider the rotor, disk and balancing element together, the equations of motion in the Ox and Oy directions can be expressed as

$$m\{(\ddot{x} - 2\omega\dot{y} - \omega^2 x) - \omega^2\delta\} + kx + m_b\{(\ddot{x} - 2\omega\dot{y} - \omega^2 x) - a(\dot{\psi} + \omega)^2 \cos\psi - a\ddot{\psi}\sin\psi\} = 0, \quad (1)$$

$$m(\ddot{y} + 2\omega\dot{x} - \omega^2 y) + ky + m_b\{(\ddot{y} + 2\omega\dot{x} - \omega^2 y) - a(\dot{\psi} + \omega)^2 \sin\psi + a\ddot{\psi}\cos\psi\} = 0. \quad (2)$$

As the balancing element of radius r rolls on the guide of radius $(a + r)$ to the angular position ψ, it rotates through the angle $-a\psi/r$ in the reference frame. The

moment equation for the rolling element about the contact point therefore becomes

$$\{m_b a\ddot{\psi} + m_b(\ddot{y} + 2\omega\dot{x} - \omega^2 y)\cos\psi - m_b(\ddot{x} - 2\omega\dot{y} - \omega^2 x)\sin\psi\}r + J_b(a/r)\ddot{\psi} = 0. \tag{3}$$

Equations (1)–(3) have steady state solutions for x, y and ψ which are independent of time. In the rotating frame, these time independent solutions can be expressed as

$$x_s = \frac{\Omega^2(\delta + va\chi_0)}{\{1 - (1 + v)\Omega^2\}}, \qquad y_s = 0, \qquad \psi_s = 0 \text{ or } \pi, \tag{4–6}$$

where

$$\Omega = (m\omega^2/k)^{1/2}, \qquad v = m_b/m, \qquad \chi_0 = \cos\psi_s. \tag{7–9}$$

The variables Ω and v, defined in equations (7) and (8), are termed non-dimensional speed and mass ratio, respectively. Equations (6) indicate that the balancing element has two relative rest positions at $\psi_s = 0$ and $\psi_s = \pi$ inside the guide. For these balancing element positions, the corresponding steady displacement (x_s, y_s) of the disk in the rotating frame are given in equations (4) and (5). These time independent solution sets represent the two possible whirling motions of the rotor with the balancing element at a relative rest position inside its guide. The parameter χ_0, which takes the values of 1 for $\psi_s = 0$ and -1 for $\psi_s = \pi$, as indicated in equations (6) and (9), is introduced to unify the dynamics of the system about these rest positions in a single analysis.

Equations (4) and (5) show that, under the steady conditions, the disk center whirls in a circular orbit of radius x_s which becomes infinite when $\Omega = 1/\sqrt{(1 + v)}$. Thus, the presence of the balancing element increases the system mass and thereby reduces the critical whirling speed. The influence of the balancing device on the unbalance whirling motion of the rotor can be studied by comparing $|x_s|$ with its value for the special case $v = 0$. However, for such a comparison to be physically meaningful, the perturbed motion of the system from the steady state must be stable. Thus, it is necessary to study the stability of the two possible steady states corresponding to the balancing element positions at $\psi_s = 0$ and $\psi_s = \pi$. As stated earlier, the two values of the parameter χ_0 can be used to identify these steady states in the stability analysis.

4. PERTURBED MOTION FROM STEADY STATE

The general motion of the system can be considered as a perturbation of the steady whirling motion. Using the perturbed co-ordinates $\Delta x = x - x_s$, $\Delta y = y - y_s$ and $\Delta\psi = \psi - \psi_s$, equations (1)–(3) can be rewritten as

$$(1 + v)\Omega^2\{\Delta x'' - 2\Delta y' - \Delta x\} + \Delta x + va\chi_0\Omega^2\{1 - (1 + \Delta\psi')^2\cos\Delta\psi - \Delta\psi''\sin\Delta\psi\} = 0, \tag{10}$$

$$(1 + v)\Omega^2\{\Delta y'' + 2\Delta x' - \Delta y\} + \Delta y - va\chi_0\Omega^2\{(1 + \Delta\psi')^2\sin\Delta\psi - \Delta\psi''\cos\Delta\psi\} = 0, \tag{11}$$

$$(1+\alpha)a\chi_0\Delta\psi'' + (\Delta y'' + 2\Delta x' - \Delta y)\cos\Delta\psi$$
$$- (\Delta x'' - 2\Delta y' - \Delta x)\sin\Delta\psi + x_s \sin\Delta\psi = 0, \tag{12}$$

where $\alpha = (J_b/m_b r^2)$ is a non-dimensional shape factor of the rolling element. The prime in equations (10)–(12) denotes differentiation with respect to the non-dimensional time ωt. Since $\psi = \psi_s + \Delta\psi$, the expressions $\cos\psi = \chi_0 \cos\Delta\psi$ and $\sin\psi = \chi_0 \sin\Delta\psi$ are substituted into equations (1)–(3) for the derivation of equations (10)–(12).

5. STABILITY ANALYSIS

When Δx, Δy and $\Delta\psi_s$ are small, equations (10)–(12) can be linearized to the first order of Δ and these linearized equations can be used to study the stability of the two possible relative rest positions corresponding to $\chi_0 = \pm 1$. Substitution of the modal solutions $\Delta x = A_x\, e^{s\omega t}$, $\Delta y = A_y\, e^{s\omega t}$ and $a\Delta\psi = \chi_0 A_\psi\, e^{s\omega t}$ into the linearized equations gives

$$\{1 - (1+v)\Omega^2 + (1+v)\Omega^2 s^2\}A_x - 2(1+v)\Omega^2 s A_y - 2v\Omega^2 s A_\psi = 0, \tag{13}$$

$$2(1+v)\Omega^2 s A_x + \{1 - (1+v)\Omega^2 + (1+v)\Omega^2 s^2\}A_y + v\Omega^2(s^2-1)A_\psi = 0, \tag{14}$$

$$2sA_x + (s^2-1)A_y + \{(1+\alpha)s^2 + \chi_0 x_s/a\}A_\psi = 0, \tag{15}$$

and the frequency equation can be obtained from equations (13)–(15) as,

$$C_0 s^6 + C_1 s^4 + C_2 s^2 + C_3 = 0, \tag{16}$$

where

$$C_0 = (\chi_0\lambda/v_c)u^2(1-u), \qquad C_1 = (\chi_0\lambda/v_c)\{2u(1-u^2) + v_c u\} + u^3, \tag{17, 18}$$

$$C_2 = (\chi_0\lambda/v_c)\{(1-u)^3 + v_c(1+3u)\} + 2u^2(1+u), \qquad C_3 = u(1-u)^2, \tag{19, 20}$$

$$u = (1+v)\Omega^2, \qquad v_c = v/\{1+\alpha(1+v)\}, \qquad \lambda = va/\delta. \tag{21–23}$$

The frequency equation (16) has terms in even powers of s only and it can be reduced to a cubic equation in p using the substitution $p = -s^2$. For stability of the perturbed motion all three roots of the cubic equation $C_0 p^3 - C_1 p^2 + C_2 p - C_3 = 0$ must be real and positive and the stable system has three vibratory modes in the rotating frame at frequencies $\omega\sqrt{p}$. From equations (13)–(15), the corresponding vibration modes can be simplified to

$$\Delta x = a_x \cos\omega\sqrt{pt}, \qquad \Delta y = a_y \sin\omega\sqrt{pt}, \qquad a\Delta\psi = \chi_0 a_\psi \sin\omega\sqrt{pt},$$

where

$$a_x = 2u\sqrt{p}, \qquad a_y = u\{(1-u) + (1+2u)p - up^2\},$$
$$a_\psi = \{(1+v)/v\}\{(1-u)^2 - 2u(1+u)p + u^2p^2\}.$$

The system has three natural frequencies and modes in the rotating frame. For small perturbed motion, the positions of the rotor center and the balancing

element center in the rotating frame can be expressed by their co-ordinates as $x = x_s + a_x \cos \omega\sqrt{pt}$, $y = a_y \sin \omega\sqrt{pt}$, $x_b = x_s + \chi_0 a + a_x \cos \omega\sqrt{pt}$ and $y_b = (a_y + a_\psi) \sin \omega\sqrt{pt}$. The constant terms in the above co-ordinate expressions represents synchronous circular whirling motions in the stationary frame. However, the time-dependent components in these expressions represent a superposition of two circular orbits in the stationary frames at frequencies $\omega(1 \pm \sqrt{p})$. The corresponding radii of the perturbed orbits of the rotor center and the balancing element center in the stationary frame are $(a_x \pm a_y)/2$ and $(a_x \pm a_y \pm a_\psi)/2$, respectively. Thus, even when the system is stable, it remains sensitive to disturbances at these six additional frequencies in the stationary frame.

For system stability, all three roots of the equation $C_0 p^3 - C_1 p^2 + C_2 p - C_3 = 0$ for p must be positive. A method to analyze this stability condition from this type of equation for the special case $\alpha = 0$ is reported in the previous study [9]. In this method the frequency equation is expressed in the form

$$\frac{\chi_0 \lambda p}{v_c} = \frac{u^3 p^2 - 2u^2(1+u)p + u(1-u)^2}{u^2(1-u)p^2 - \{2u(1-u^2) + v_c u\}p + \{(1-u)^3 + v_c(1+3u)\}} \tag{24}$$

and the intersections of the graphs of the linear and biquadratic functions of the variable p on either sides of equation (24) are then investigated. The variables v_c and v in equation (24) become identical in the special case $\alpha = 0$ discussed earlier [9]. However, when $\alpha \neq 0$, this new variable v_c, defined in equation (22), increases steadily with v and approaches the limit $1/\alpha$ as v tends to infinity.

For stability, the graphs of the linear and the biquadratic functions of p in equation (24), must intersect at three points which have positive abscissa. The special case where the straight line touches the biquadratic curve and interesect it again represents the boundary state that separates the stability and instability of the system, provided that the common points between the graphs have positive abscissa. The graph of the biquadratic function of p on the right side of equation (24) depends on the relative positions of its poles and zeros on the p-axis depends on the assumed parameters u and v_c in the coefficients of the biquadratic function.

For a chosen u and v_c, the poles and zeros of this biquadratic function are real. Further, the two zeros and one pole of this function remain positive whereas the other pole becomes negative in the speed range $1 < u < 1 + w$ where w is the positive root of equation $w^3 - 3v_c w - 4v_c = 0$. For a presumed v_c, the dependence of this poles–zeros location on u can be categorized into three groups based on the speed ranges $u < 1$, $1 < u < 1 + w$ and $u > 1 + w$. Since the biquadratic curve has three different shapes, the system stability must be investigated separately for these speed ranges.

At the stability boundary state, the straight line graph of the linear function on the right side of equation (24) touches the biquadratic curve and intersects it again at points which have positive abscissa. For a chosen v_c, an examination of this boundary state yields the limiting values of the slope of the straight line that touches the biquadratic curve in terms of u. Consequently, when v_c and u are known, the limiting values of λ at the stability boundary state for each balancing element position can be determined. The results of the stability analysis of the two

TABLE 1

Stability of steady motions for a chosen mass ratio

Speed range	Position $\psi_s = 0$	Position $\psi_s = \pi$
$u < 1$	Stable	Unstable
$1 < u < 1 + w$	Unstable	Stable: $\lambda \leqslant \lambda_1$ Unstable: $\lambda > \lambda_1$
$1 + w < u$	Unstable	Stable: $\lambda \leqslant \lambda_1$ or $\lambda \geqslant \lambda_2$ Unstable: $\lambda_1 < \lambda < \lambda_2$

steady motions with the balancing element at $\psi_s = 0$ and $\psi_s = \pi$ for the three speed ranges are shown in Table 1.

At sub-critical speeds ($u < 1$), the only stable position of the balancing element is $\psi_s = 0$. However, when $u < 1$, equation (4) shows that the balancing element at this position can only increase the resulting system unbalance and consequently the automatic balancing device is undesirable for this speed range. In the supercritical speed range ($u > 1$), the second position $\psi_s = \pi$ of the balancing element is stable when λ satisfies certain conditions shown in Table 1. For the explicit statement of the stability conditions in the supercritical speed range, it is necessary to subdivide this speed range into the low supercritical ($1 < u < 1 + w$)

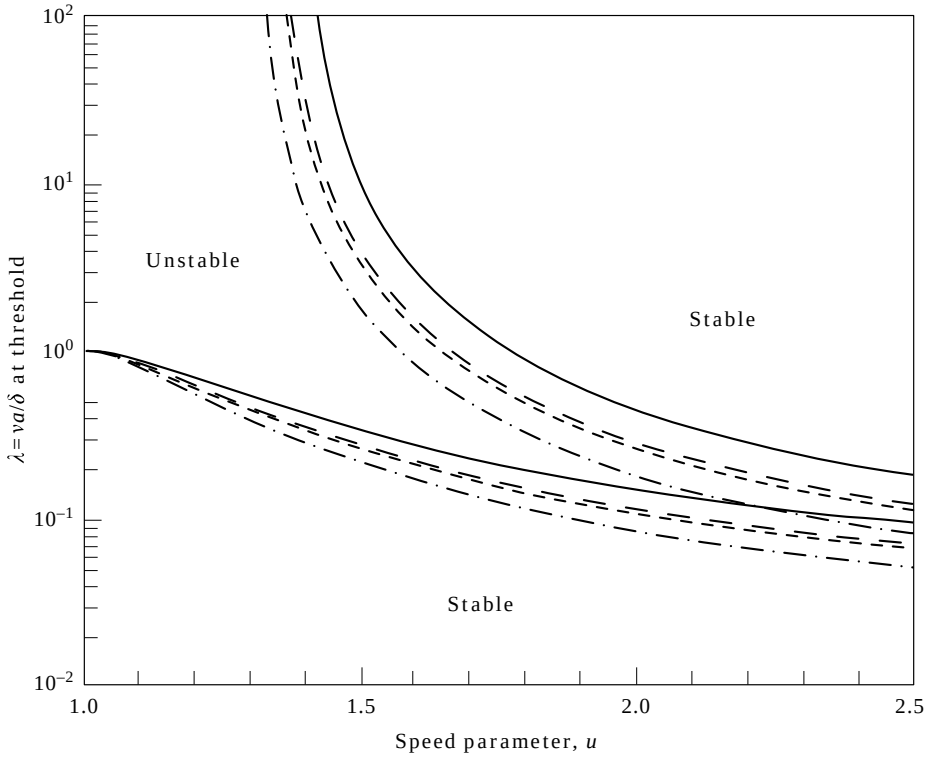

Figure 2. Stability boundaries in the (u, λ) plane for various balancing element geometries, $v = 0{\cdot}01$: ——, $\alpha = 0$; — — —, $\alpha = 0{\cdot}4$; – – – –, $\alpha = 0{\cdot}5$; ·–·–·–·, $\alpha = 1{\cdot}0$.

and high super-critical speed ranges ($u > 1 + w$) as in Table 1. It must be noted that for a chosen v_c, the limiting values λ_1 and λ_2 corresponding to the stability boundary state can be tabulated as a function of u. Using the condition that the frequency equation $C_0p^3 - C_1p^2 + C_2p - C_3 = 0$ has coincident roots at the stability boundary state, it can be shown that these limiting values λ_1 and λ_2 approach v_c as u increases to infinity.

The stability boundary states corresponding to $v = 0{\cdot}01$ are shown graphically in Figure 2 for five values of α. Here, $\alpha = J_b/m_br^2$, represents the geometric shape of the rolling element. The ideal case $\alpha = 0$, which corresponds to a small roller with its entire mass concentrated at its axis, simulates the smooth contact condition considered in the earlier analysis [9]. The other values of α in Figure 2 represent the spherical, cylindrical and ring shaped balancing elements. It can be observed that the limiting values of λ in the supercritical speed range decreases as α increases.

When the balancing element position at $\psi_s = \pi$ is stable, its effect on the unbalance vibration can be deduced by comparing the steady whirling amplitude $|x_s|$ in equation (4) with its special value corresponding to $v = 0$. Such an investigation shows that the balancing element at $\psi_s = \pi$ reduces the unbalance whirling amplitude of the rotor when $0 < \lambda < 2 + v$ and $\Omega^2 > [(1 + |1 - \lambda|)/(1 + v + |1 - \lambda|)]$. The vibration reduction with the device is also possible within the speed range $[(\lambda)/(\lambda + v)] < \Omega^2 < [(\lambda - 2)/(\lambda - 2 - v)]$ for λ larger than $2 + v$. It can be noticed that when $\lambda = 1$ the system unbalance is completely neutralized

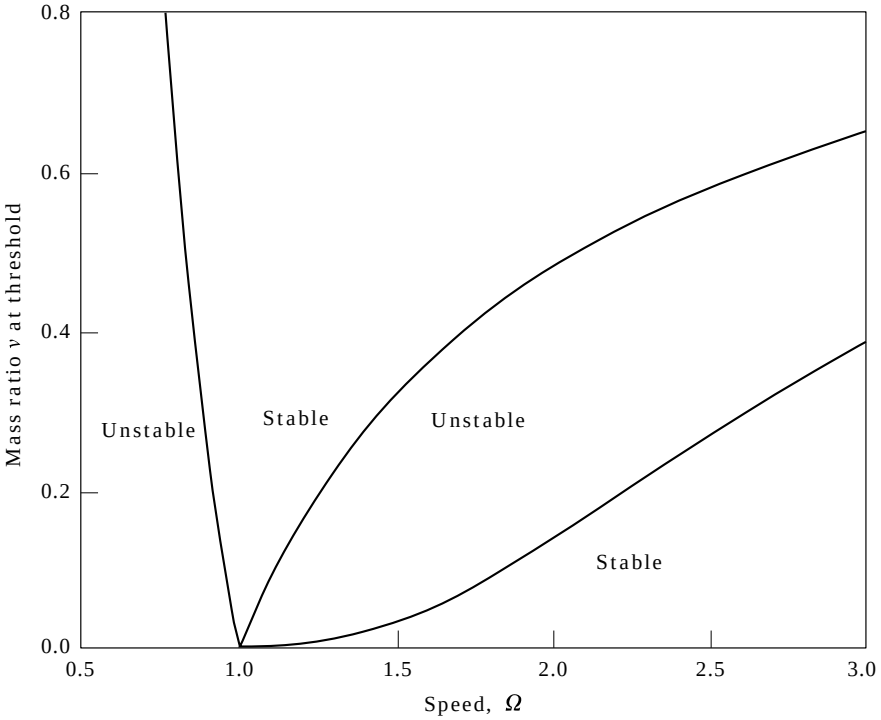

Figure 3. Stability boundaries in the (Ω, v) plane for $\alpha = 0$ and $\lambda = 1{\cdot}0$.

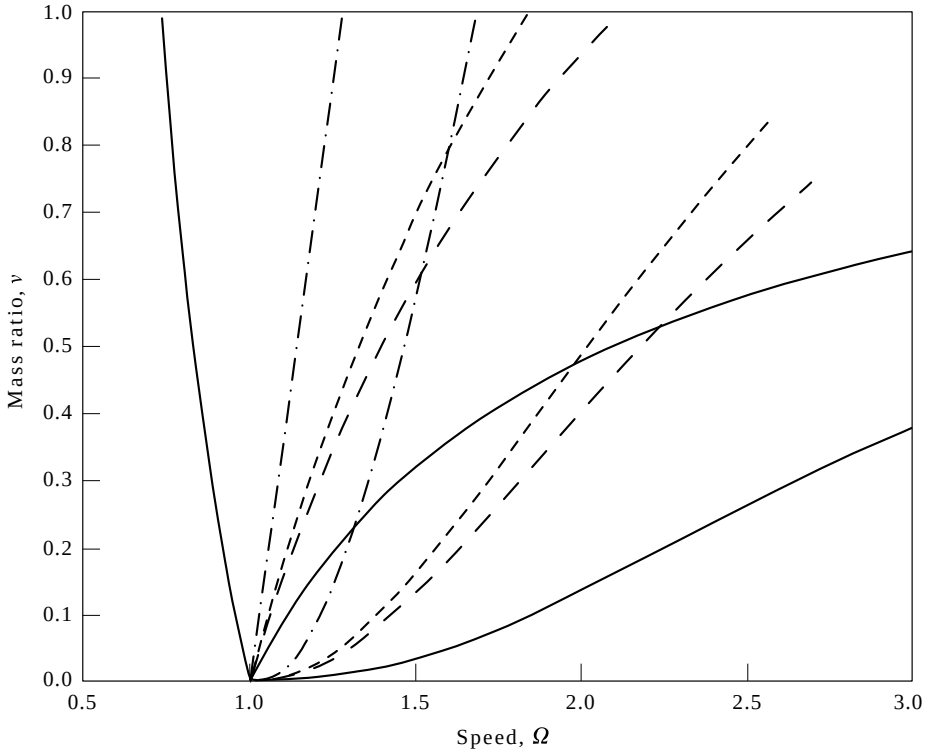

Figure 4. Variation of stability boundaries in the (Ω, v) plane with the balancing element geometry, $\lambda = 1{\cdot}0$: ——, $\alpha = 0$; — — —, $\alpha = 0{\cdot}4$; – – – –, $\alpha = 0{\cdot}5$; ·–·–·–·, $\alpha = 1{\cdot}0$.

within the speed ranges for which the rest position $\psi_s = \pi$ of the balancing element is stable. Additional information on the stability of the balancing element position $\psi_s = \pi$ when $\lambda = 1$ is useful to the optimum design of the balancing device which can completely neutralize the unbalance vibration.

When $\lambda = 1$, the system stability equation (24) can be rewritten as

$$\frac{p}{v_c} = \frac{u(1+u)p^2 - (1+4u+2u^2)p + u(u-1)}{u^2p^2 - 2u(1+u)p + (u-1)^2}. \tag{25}$$

For stability of the balancing element position $\psi_s = \pi$, the graphs of the linear and biquadratic functions of p on either sides of equation (25) must intersect at three points with positive abscissa. The coefficients of the biquadratic function depend on u. Since $u > 1$, the poles and zeros of the biquadratic function in equation (25) are real and both zeros lie in between the poles. At the stability boundary state corresponding to an assumed u greater than unity, two straight lines can be drawn to touch the biquadratic curve. From the slopes of the common tangent, the limiting values v_1 and v_2 of v can be tabulated as functions of u for $u > 1$. Further, the stable speed ranges of the balancing element position can be seen from the graphical interpretation as $v > v_2$ and $v < v_1$, respectively.

Since Ω is a better non-dimensional parameter than u to represent rotor speed, the stability boundaries $u = 1$, $v > v_2(u)$ and $v < v_1(u)$ in the (u, v) plane can be

transformed to the (Ω, v) plane using the relation $\Omega = 1/\sqrt{(1+v)}$. The stability boundaries corresponding to the case $\lambda = 1$, which represents the complete unbalance neutralization is shown in Figure 3. As α increases, the supercritical speed range of instability of the balancing element at $\psi_s = \pi$ reduces and moves towards $\Omega = 1$. Here, the unstable speed range reduction is a favorable influence of rolling motion of the balancing element whereas the movement of this speed range towards $\Omega = 1$ is unfavorable. However, Figure 4 can be used to interpret the effect of the rolling motion of the balancing element and to extract useful information for the automatic balancing device design.

6. DISCUSSION

The balancing device used in Lindell's experiment [6] has several rollers whose positions inside the groove during the steady whirling motion of the system modify the effective rotor unbalance. When the contact friction is small, the balance of the forces acting on these balancing elements during the steady state indicates that these elements must cluster at the extremities of the groove diameter which passes through the mass center of the rotor disk. Since the effect of this distribution on the balancing elements is equivalent to that of a single roller, a single element is used in the present theoretical model. Since the flexibility of the rotor shaft plays an important role in the balancing mechanism of this device, a three-degree-of-freedom system model in the rotating reference frame is necessary for the present investigation.

Corresponding to the two roller positions $\psi_s = 0$ and $\psi_s = \pi$ inside the groove, the system has two possible whirling modes, expressed in equations (4)–(6). The balancing element mass at these rest positions reduces the system natural frequency to $\sqrt{k/(m+m_b)}$. In the sub-critical speed range $\Omega < 1\sqrt{(1+v)}$, the first position ($\psi_s = 0$) of the balancing element is stable. However, since the balancing element at $\psi_s = 0$ increases the effective rotor unbalance, the automatic balancing device can only worsen the unbalance whirling motion of the rotor in the sub-critical speed range.

In the super-critical speed range $\Omega > 1/\sqrt{(1+v)}$, Table 1 indicates that the second position ($\psi_s = \pi$) can sometimes become stable. Equation (4) shows that when $0 < \lambda < 2 + v$ and $\Omega^2 > [(1 + |1-\lambda|)/(1 + v + |1-\lambda|)$, the balancing element at this position reduces the unbalance whirling motion of the rotor shaft. This range of λ contains the design target value $\lambda = 1$ for complete unbalance neutralization. Thus, it is important to investigate the conditions for the stability of this balancing element position. The conditions for the stability of the second position for the special case $v = 0{\cdot}01$ is shown in Figure 2. Here, the boundary states are represented by the curves $\lambda = \lambda_1(u)$ and $\lambda = \lambda_2(u)$. The lower boundary curve $\lambda = \lambda_1(u)$ increases very slowly from $\lambda = 1$ and then begins to decrease to v_c as u increases to infinity. The upper boundary curve $\lambda = \lambda_2(u)$, which is defined for $u > 1 + w$, decreases steadily from infinity to v_c as u increases from $1 + w$ to infinity. Thus, the stability results, shown in Figure 2 must be studied separately for four λ ranges, namely (1) $\lambda < v_c$, (2) $v_c < \lambda \leqslant 1$, (3) $1 < \lambda \leqslant [\lambda_1(u)]_{max}$ and (4) $\lambda > [\lambda_1(u)]_{max}$.

When $\lambda < v_c$, the balancing element at the second position must remain stable for all $u > 1$. Since v_c is small, the values of λ in this range are not significant enough to change the rotor unbalance appreciably and consequently this λ range will be of theoretical interest only. For any chosen λ in $v_c < \lambda \leqslant 1$, Figure 2 shows that the second rest position becomes unstable for a certain speed range. When λ lies between unity and the maximum value of $\lambda_1(u)$, the second position is stable within two speed ranges. However, in this case, the first stability range commences at a u greater than unity. For the fourth case correpsonding to sufficiently large λ, the second position is stable when the speed exceeds that corresponding to $\lambda_2(u)$.

The automatic balancing device is useful in reducing rotor vibration when $0 < \lambda < 2 + v$ and $\Omega^2 > [(1 + |1 - \lambda|)/(1 + v + |1 - \lambda|)]$, provided that the balancing element at the second position is stable. However, the stable system has three natural frequencies of perturbed vibration in the rotating reference frame. Transformation of the vibration mode from the rotating frame indicates that the stable system has six natural frequencies in the stationary frame, and consequently the balancing device is sensitive to disturbances at these six frequencies.

In the special case $\lambda = 1$, the balancing element at $\psi_s = \pi$ can completely neutralize the unbalance rotor vibration when the system is stable at the rotor speed. The stability of the system for this special case is shown in Figure 4. In this graph the stable speed ranges of three types of rolling elements are compared with that corresponding to the smooth contact ($\alpha = 0$). The result shows that the rolling of the balancing element shortens the speed range of system instability, and consequently it favorably reduces the vibration of hand-held power tools within a wider speed range. However, the balancing element rolling also brings the unstable speed range towards the rotor critical speed, which is undesirable. Fortunately, this undesirable influence becomes significant only when the balancing element mass is comparable to the rotor mass. Since the balancing element mass is less than 20% of the system mass, the favorable influence of the rolling motion of the element on the stability predominates. Thus, in a carefully designed balancer, the rolling of the balancing element has a positive influence on vibration suppression.

The prototype of the balancing device consists of multiple rollers which are free to roll inside a sealed cylindrical ball–race unit filled partially with oil. The lubricating film between the roller and its guide reduces the contact friction and behaves like a viscous damper at high sliding velocities. During the motion of the roller from its initial position to its steady state position, the viscous damping in the oil film is expected to play a significant role in nullifying the relative motion between the roller and its guide. It is also known, that under certain conditions, this type of viscous damping between the roller and its guide in the rotating frame could destabilize the initial motion of the roller. The impact between the balls also enhances the damping effect during the initial motion of the system. A critical study of this viscous and impact influence on the initial motion of the roller is beyond the scope of the present investigation.

7. CONCLUSIONS

The influence of the rolling motion of the balancing element due to contact friction on the unbalance vibration of the rotor is investigated in a rotating reference frame using a three-degree-of-freedom system model. The balancing element rolling reduces the unstable speed range of the system and thereby increases the effective speed range of the balancing device. When the balancing element mass is significantly large, the rolling effect brings the unstable speed range towards the rotor critical speed. Since the balancing element mass is less than 20% of the rotor mass, the rolling effect can be used to enhance the effectiveness of the automatic balancing in a carefully designed balancing device.

REFERENCES

1. D. Washerman, D. Badger, T. E. Doyle and L. Marsolis 1974 *Journal of American Society of Safety Engineers* **19**, 38–43. Industrial vibration—an overview.
2. M. J. Griffin 1990 *Handbook of Human Vibration*. London: Academic Press.
3. R. Gurram, S. Rakheja and A. J. Brammer 1995 *Journal of Sound and Vibration* **180**, 437–458. Driving-point mechanical impedance of the human hand–arm system: synthesis and model development.
4. C. W. Suggs and C. F. Abrams, Jr. 1983 in *Proceedings of the* 27*th Annual Meeting of the Human Factors Society*. Vibration isolation of power tools operators.
5. R. Gurram, S. Rakheja and G. J. Gouw 1994 *International Journal of Industrial Ergonomics* **13**, 217–234. Vibration transmission characteristics of the hand–arm and gloves.
6. H. Lindell 1996 *Central European Journal of Public Health* **4**, 43–45. Vibration reduction on hand–held grinders by automatic balancing.
7. J. P. Den Hartog 1956 *Mechanical Vibrations*. New York: McGraw Hill Book Company Inc.; fourth edition.
8. A. Tondl 1965 *Some Problems in Rotor Dynamics*. London: Chapman and Hall.
9. C. Rajalingham, R. B. Bhat and S. Rakheja 1998 *International Journal of Mechanical Sciences*, **9,** 825–834. Automatic balancing of flexible vertical rotors using a guided ball.

APPENDIX: NOMENCLATURE

a	radius of the path of the balancing element center of mass
a_x, a_y and a_ψ	coefficients of perturbation modes
A_x, A_y, A_ψ	complex coefficients of perturbation modes
C_0, C_1, C_2 and C_3	coefficients of the frequency equation
J_b	moment of inertia of balancing element
k	rotor stiffness
m	rotor mass
m_b	balancing element mass
p	$p = -s^2$
r	radius of balancing element
s	non-dimensional complex frequency
t	time
u	defined in equation (21)
(x, y)	co-ordinates of rotor center in rotating frame
(x_s, y_s)	steady state solutions for (x, y)
$(\Delta x, \Delta y)$	perturbation in (x, y)
α	$\alpha = J_b/m_b r^2$

δ	residual unbalance eccentricity
λ	$\lambda = va/\delta$
λ_1, λ_2	λ at stability boundary state
v	mass ratio, $v = m_b/m$
v_c	v_c defined in equation (22)
v_1, v_2	limiting values of v
χ_0	$\chi_0 = \cos \psi_s$
ψ	balancing element position
ψ_s	steady state solution of ψ
$\Delta\psi$	perturbation in ψ
ω	rotor speed
Ω	defined in equation (7)
$( )'$	derivative of ( ) with respect to time